

# A Molecular View on the Role of Cholesterol upon Membrane Insertion, Aggregation, and Water Accessibility of the Antibiotic Lipopeptide Trichogin GA IV As Revealed by EPR

Victoria N. Syryamina,<sup>†</sup> Marta De Zotti,<sup>‡</sup> Cristina Peggion,<sup>‡</sup> Fernando Formaggio,<sup>‡</sup> Claudio Toniolo,<sup>‡</sup> Jan Raap,<sup>\*,§,⊥</sup> and Sergei A. Dzuba<sup>†,||</sup>

<sup>†</sup>Institute of Chemical Kinetics and Combustion, Russian Academy of Sciences, 630090 Novosibirsk, Russia

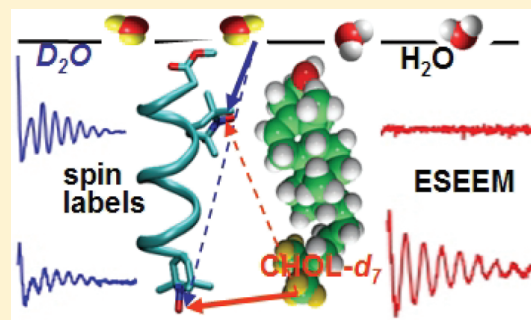
<sup>‡</sup>ICB, Padova Unit, CNR, Department of Chemistry, University of Padova, 35131 Padova, Italy

<sup>§</sup>Leiden Institute of Chemistry, Gorlaeus Laboratories, University of Leiden, 2300 RA Leiden, The Netherlands

<sup>||</sup>Department of Physics, Novosibirsk State University, 630090 Novosibirsk, Russia

## S Supporting Information

**ABSTRACT:** Trichogin GA IV is a membrane-active lipopeptide, the antibiotic activity of which was proposed to be based on its capability to induce leakage due to formation of pores into the bacterial cell membrane. However, less attention has been paid to its biological selectivity, i.e., discrimination between bacterial versus cholesterol containing (mammalian) membranes. This is the reason which motivated us to study the role of cholesterol on penetration of the peptide into the membrane and formation of water channels. The ESEEM technique was used to measure the modulation amplitudes for TOAC spin-labeled trichogin GA IV peptide analogues in hydrated membranes of phosphatidylcholine (PC) lipid in the presence of 50 mol % cholesterol-*d*<sub>7</sub>. From the interaction between the nitroxide spin-label and the nearby located deeply membrane inserted deuterons, the N-terminus was found to be positioned at the core of the membrane. Separately, ESEEM measurements for the FTOAC-8 labeled peptide, but in D<sub>2</sub>O hydrated cholesterol/PC membranes, provide strong evidence for the polar C-terminus situated near the membrane surface. The apparently too high modulation amplitude measured for the buried FTOAC-1 label is likely attributed to the presence of peptide associated water. In cholesterol depleted membrane, however, the long axes of the helical molecules are found oriented parallel to the membrane surface even at high peptide concentration. Continuous wave EPR spectroscopy indicates that, for cholesterol containing membrane, peptide insertion is accompanied by self-aggregation of parallelly aligned transmembrane peptide molecules, while for cholesterol lacking membranes they are monomolecularly distributed. Thus, cholesterol tends to stabilize the transmembrane peptide aggregate.



## INTRODUCTION

A number of bacterial and fungal species produce lipopeptide antibiotics<sup>1</sup> with short linear or cyclic chains. In a well-defined range of concentrations they function by selectively targeting microbial cell membranes. However, above a certain threshold concentration they become harmful to mammalian cells despite the latter being endowed with cholesterol (CHOL) stabilized membranes. Toxic effects of antibiotics are generally believed to be caused by disruption of the eukaryotic cell membranes and subsequent leakage of the cell contents. However, little is known about the underlying molecular mechanism of this process. In this work, we investigated the molecular role of CHOL on the membrane leakage induced by the antibiotic lipopeptide trichogin GA IV.

This 10-mer peptide is produced by fungi of the genus *Trichoderma* and is characterized by a fatty acyl group attached to the N-terminus and an 1,2-aminoalcohol at the C-terminus.<sup>2</sup>

Inspections of crystal<sup>3,4</sup> and NMR-solution<sup>5</sup> data for trichogin GA IV and selected analogues show a mixed 3<sub>10</sub>-/ $\alpha$ -helix.

Fluorescent-labeled trichogin GA IV molecules added to the outside of vesicular membranes [egg phosphatidylcholine (PC)/50% CHOL] were found uniformly distributed at both sides of the bilayer. This finding demonstrates the possibility of peptide translocation across the membrane at concentrations where leakage occurs.<sup>6–8</sup> At higher concentration, the peptide molecules are more deeply inserted into the hydrophobic inner core of the membrane. The level of membrane leakage is linearly correlated with the concentration of membrane-bound aggregates. Peptide-induced membrane leakage was suggested

**Received:** February 20, 2012

**Revised:** April 30, 2012

**Published:** April 30, 2012



to be based on a pore-, rather than by a detergent-, carpet- or toroidal-like mechanism.<sup>6</sup>

The electron spin echo envelope modulation (ESEEM) technique allows the examination of different water accessibilities for peptide-attached spin-labels at different levels of membrane insertion.<sup>9–17</sup> Applicability of this technique originates from the anisotropic hyperfine interactions (hfi) as well as the nuclear quadrupole interactions between the unpaired electron of a spin-label with the nearby located magnetic deuterium nuclei of D<sub>2</sub>O hydrated membranes.<sup>9–18</sup> Since water molecules are less abundant in the hydrophobic core of the membrane, the amplitude of the ESEEM spectrum depends on the depth of the peptide label position relative to the membrane surface. Thus, the water-induced modulation amplitudes observed for spin-labels attached to different positions of the peptide chain provide an indicator for the orientation as well as the penetration depth of the membrane bound peptide. This method was exploited to investigate the membrane-bound state of trichogin GA IV,<sup>10,16</sup> zervamicin IIA,<sup>15</sup> and alamethicin.<sup>17</sup>

Recently, it was shown that in 2-oleoyl-1-palmitoyl-*sn*-glycero-3-phosphocholine (POPC) and 1,2-dipalmitoyl-*sn*-glycero-3-phosphocholine (DPPC) membranes at high peptide concentration trichogin GA IV changes its orientation from the in-plane bound state to a transmembrane disposition.<sup>16</sup> From dynamic information the peptide molecules were suggested to self-associate to head-to-head transmembrane dimers, the length of which would match the thickness of the double layer. However, most of the previous EPR results were achieved by using lipid membrane systems in the absence of CHOL.

To obtain a deeper understanding on the relationship between the molecular peculiarities of the membrane-bound peptide and its antibiotic and toxic activities, it is imperative to investigate the role of CHOL on the pore-forming capability of trichogin GA IV in eggPC membranes at different peptide concentrations. From the molecular point of view, such a pore is characterized by a water-associated and membrane-inserted peptide aggregate.

In the present work, we show the usefulness of a complementary ESEEM method to investigate the role of CHOL on the insertion of the membrane-active peptide trichogin GA IV that is based on the ESEEM modulation that occurs upon interaction between the peptide attached spin-label and the deeply membrane inserted deuterated alkyl chains of the CHOL-*d*<sub>7</sub> molecules. Thus, this new method allows monitoring the spin-labels of trichogin GA IV analogues which are located at the core of the membrane. In this manner, both the orientation and immersion depth of the lipopeptide molecules are determined and compared with the data obtained from the D<sub>2</sub>O method.

Spin-labeling of the two analogues of trichogin GA IV investigated in this work was achieved by inserting a TOAC (4-amino-1-oxyl-2,2,6,6-tetramethylpiperidine-4-carboxylic acid)  $\alpha$ -amino acid at position 1 or 8 where the noncoded Aib ( $\alpha$ -aminoisobutyric acid) residues are located in the native lipopeptide sequence:

Trichogin GA IV: *n*-Oct-Aib-Gly-Leu-Aib-Gly-Gly-Leu-Aib-Gly-Ile-Lol

FTOAC-1: Fmoc-TOAC-Gly-Leu-Aib-Gly-Gly-Leu-Aib-Gly-Ile-Leu-OMe

FTOAC-8: Fmoc-Aib-Gly-Leu-Aib-Gly-Gly-Leu-TOAC-Gly-Ile-Leu-OMe

The Leu-OMe moiety is the synthetic precursor of the native C-terminal 1,2-aminoalcohol leucinol (Lol). In the analogues, the N-terminal *n*-octanoyl (*n*-Oct) group is replaced by the equally hydrophobic, but fluorescent, fluorenyl-9-methoxycarbonyl (Fmoc) group. It is known that these replacements do not alter the 3D-structural properties or the membrane activity of trichogin GA IV.<sup>19,20</sup> We selected Fmoc analogues for this lipopeptide in order to be able to study them by fluorescence spectroscopy as well.

It was already unambiguously demonstrated that the TOAC and Aib C $\alpha$ -tetrasubstituted  $\alpha$ -amino acids share strictly comparable, strong helicogenic properties.<sup>19,20</sup> The important advantage of TOAC is that its nitroxide spin-label is rigidly linked via the piperidine ring structure to the  $\alpha$ -carbon atom of the peptide backbone. It is for this reason that this residue reports more accurately on the structural peculiarities of the peptide than the much more flexible 1-oxyl-2,2,5,5-tetramethylpyrroline-3-methylmethanethiosulfide (MTSSL)/cysteine spin-label, currently extensively used in protein studies (Figure 1S, Supporting Information).

Two different experimental conditions were chosen to strictly mimic those typical of antibiotic and toxic activities, i.e. 0.5 mol % peptide/eggPC and 5.0 mol % peptide/CHOL/eggPC, respectively.

## ■ EXPERIMENTAL SECTION

**Materials and Sample Preparations.** The syntheses and characterizations of the two trichogin GA IV analogues were already described.<sup>19</sup> EggPC, the lipid extracted from egg yolk (a mixture of phosphocholine lipids composed of C16:0/18:1 lipids as the major components), and CHOL were obtained from Sigma (St. Louis, MO). Deuterated CHOL (CHOL-*d*<sub>7</sub>) was purchased from Avanti Polar Lipids (Alabaster, AL). Spin-labeled lipids, 2-oleoyl-1-palmitoyl-*sn*-glycero-3-phospho-(tempo)choline (0-PCSL) and 1-palmitoyl-2-stearoyl-(*n*-doxyl)-*sn*-glycero-3-phosphocholine (*n*-PCLS), where *n* = 5, 7, 10, 12, 14, and 16 denotes the carbon position along the acyl chain, were also obtained from Avanti Polar Lipids.

Samples were prepared according to the following procedure. First, a mixture of peptide, lipid, and, in some of the samples, CHOL was dissolved in chloroform. Then, the solvent was removed by a stream of nitrogen gas followed by evaporation *in vacuo* for 3 h. Finally, some of the samples were hydrated in D<sub>2</sub>O for 24 h at room temperature, followed by three cycles of freezing and thawing. Other samples containing CHOL-*d*<sub>7</sub> were hydrated in H<sub>2</sub>O. The water content of each sample was ~50% w/w. The molar ratio of each of the CHOL containing samples was 1:1. All peptide concentrations are given as molar percentages. 1% of each of the above-mentioned spin-labeled lipids was added to the samples for calibration purposes.

We also explored the possibility of an artifact contributing to the ESEEM signal due to H  $\rightleftharpoons$  D exchange of the peptide backbone NH protons. Initially, the peptide NH protons were fully exchanged by storage of the solution in C<sub>2</sub>D<sub>5</sub>OD at room temperature. After 4 h, the solvent was evaporated and the remaining solid was dissolved in toluene (to prevent any back-exchange). The amplitude of the ESEEM signal recorded for the peptide in frozen toluene solution was found to be very small. Thus, despite the potential presence of peptide nitrogen-linked deuterium atoms, their contributions to the ESEEM signal are extremely small compared to the signals observed for the membranes containing D<sub>2</sub>O and CHOL-*d*<sub>7</sub>.

**EPR Measurements and Modeling.** We used a Bruker ESP-580 FT EPR spectrometer equipped with a Bruker ER 4118 X-MD-5 dielectric cavity inside an Oxford Instruments CF 935 cryostat. The cryostat was cooled by a flow of cold nitrogen gas. In all measurements the temperature was kept at 78.5 K. The cavity was critically coupled in continuous-wave (CW) EPR measurements and overcoupled in electron spin echo experiments. For CW EPR, the microwave power did not exceed 0.0629 mW.

The ESEEM data were acquired using the three-pulse sequence  $\pi/2-\tau-\pi/2-T-\pi/2-\tau$ -echo with microwave pulse widths of 16 ns. The time delay  $\tau$  between the first and second pulses was fixed at 200 ns, providing a maximum of deuteron modulation. The ESEEM spectra were obtained by a scanning delay  $T$  between the second and third pulses, from 248 ns to 12  $\mu$ s, with a step of 12 ns. Unwanted echoes were eliminated by a four-step phase cycling program:  $+(0, 0, 0)$ ,  $-(\pi, 0, 0)$ ,  $-(0, \pi, 0)$  and  $(\pi, \pi, 0)$ . The magnetic field was set at the maximum of the echo-detected EPR spectrum.

The ESEEM signal  $V(T)$  depends on a relaxation process which may be considered to be independent of the modulation phenomenon. The contribution of relaxation was eliminated by processing the data of the normalized echo decay  $V_n(T)$  using the equation<sup>14</sup>

$$V_n(T) = V(T)/\langle V(T) \rangle - 1 \quad (1)$$

where  $\langle V(T) \rangle$  is a smoothed function obtained by fitting the  $\ln(V(T))$  experimental decay by a six-order polynomial function (see Figure 2S; Supporting Information). To analyze the amplitude of modulation, a cosine-Fourier transformation on  $V_n(T)$  was performed:

$$F_c(f) = \int_{t_1}^{t_2} V_n(T) \cos(2\pi ft) dt \quad (2)$$

where  $t_1 = 0.248 \mu$ s,  $t_2 = 12 \mu$ s,  $t = \tau + T + t_1$ ,  $\tau = 0.2 \mu$ s, and  $f$  is the frequency in MHz. Note that  $t_1$  is determined by the dead time and  $t_2$  by the spin relaxation resulting in the disappearance of the echo signal. Numerical Fourier transformations were performed using a homemade computer program. Note that the spectral density  $F_c(f)$  obtained in such way is an absolute value,<sup>14</sup> which may be used for comparison of different systems, irrespective of the measuring scheme and device used. The  $F_c(f)$  value in eq 2 has the dimension of time. Here, we measured it in microseconds. The peak amplitude,  $A_N$ , was determined by smooth interpolation of the background line outside of the peak into the peak area, followed by its subtraction from the maximal peak value.

The molecular structure of CHOL was extracted from Spartan (Wave function Inc., Irvine, CA), and the helical model of the spin-labeled peptide was built using the Hyperchem software (Hypercube Inc., Gainesville, FL).

## RESULTS

**Role of CHOL on Peptide Membrane Insertion.** To study the role of CHOL on the immersion depths of FTOAC-1 and FTOAC-8 at two different peptide concentrations, we investigated samples with and without the presence of CHOL. First, we describe the results obtained by using samples of peptide analogues in hydrated CHOL- $d_7$ /eggPC/H<sub>2</sub>O membranes as well as in D<sub>2</sub>O hydrated CHOL/eggPC membranes (Figure 1).

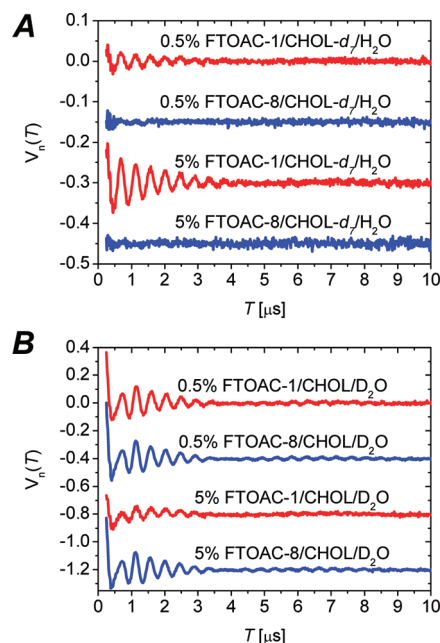


**Figure 1.** Normalized ESEEM signals decays  $V_n(T)$  for the spin-labeled analogues of trichogin GA IV in eggPC (A) with CHOL- $d_7$  and hydrated by H<sub>2</sub>O and (B) with CHOL and hydrated by D<sub>2</sub>O (for convenience, the spectra are shifted downward by 0.2).

The ESEEM signals shown in Figure 1 oscillate with a frequency of about 2.2 MHz, that is, the resonance frequency of deuterons at the X band. Panel A exhibits an intense deuterium modulation for the 5 mol % FTOAC-1 sample, while for the 0.5 mol % FTOAC-1 sample the observed modulation is not significant. Meanwhile, modulations are absent for samples prepared with FTOAC-8 at both low and high peptide concentrations.

Typical examples of cosine Fourier transformations of the normalized ESEEM decays are depicted in Figure 2A. In all cases we observed a peak amplitude  $A_N$  which is split into a doublet of amplitude  $\Delta$  due to the quadrupole interaction between the electron spin and the deuterium nuclei.<sup>14</sup> The peak amplitude is larger for the FTOAC-1 than for the FTOAC-8 nitroxide spin-labels for 5 mol % samples. This finding implies a more deeply inserted N-terminus of the peptide into the membrane. The level of peptide insertion into the membrane can be determined more precisely by using a calibration curve ( $A_N$  as a function of the different lipid carbon positions).

The calibration curve for CHOL- $d_7$ /eggPC/H<sub>2</sub>O membranes is obtained from the Fourier transform spectra of a set of nitroxide spin-labeled lipids (the original signal decays are shown in Figure 4S, Supporting Information). In Figure 3A, the  $A_N$  values are plotted versus different lipid label positions ( $n = 0, 5, 7, 10, 12, 14$ , and 16). In Figure 3B, an analogous plot is reported for the same set of spin-labeled lipids, but for samples of CHOL/eggPC/D<sub>2</sub>O, which are used to determine the proximity of peptide spin-labels to the polar membrane surface. It is worth noting that the behavior of the two data sets is opposite. In the latter case, values obtained for the lipid spin-labels near the membrane surface are large, decreasing monotonously to the zero value above the 10th-carbon position, while in the former case the  $A_N$  amplitudes are zero up to the seventh-carbon position and monotonously increase in the membrane interior.



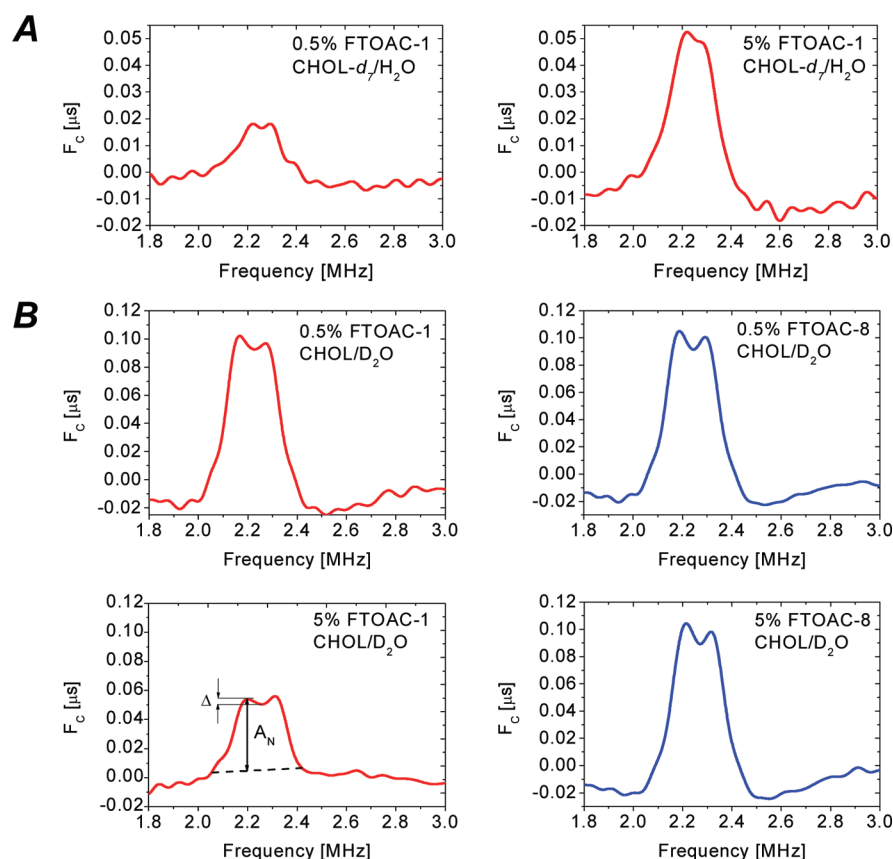


**Figure 2.** (A) A typical cosine-Fourier transformation spectra for FTOAC-1 at different peptide concentrations in eggPC/CHOL- $d_7$ /H $_2$ O. (B) Cosine-Fourier transformation spectra for spin-labeled peptides at different peptide concentrations in eggPC/CHOL/D $_2$ O. The  $A_N$  and  $\Delta$  parameters are related to free (non-hydrogen-bonded) D $_2$ O molecules situated near the spin-label at 0.5–1 nm.

For 5 mol % FTOAC-1 in CHOL- $d_7$ /eggPC/H $_2$ O membranes, much larger  $A_N$  values are shown compared to those of FTOAC-8 (Figure 3A), while in Figure 3B these data are reversed. Thus, the TOAC-8 spin-label is situated near the headgroup region of the lipid bilayer, while TOAC-1 is more deeply membrane inserted, i.e., near the level of the 10th-lipid carbon position. In Figure 3B, however, the apparent insertion level of TOAC-1 in the D $_2$ O hydrated membrane is found at the eighth-lipid carbon position. It is worth noting that the  $A_N$  value obtained for the D $_2$ O hydrated membrane is not only dependent on the presence of water natural abundance in the membrane, but it might be also influenced by the presence of locally peptide-associated water. Thus, the discrepancy between the too high  $A_N$  value in the D $_2$ O hydrated membrane is most likely attributed to an increased level of water molecules near TOAC-1.

To study the CHOL dependence on the penetration of peptides, ESEEM spectra were measured for samples with and without the presence of CHOL at different label positions and also at different peptide concentrations. The peak amplitudes,  $A_N$ , obtained for the spin-labeled peptides in D $_2$ O hydrated membranes are collected in Table 1. For the CHOL-free membrane, the relatively high peak amplitudes are approximately independent of both label position and peptide concentration (see also Figure 3S, Supporting Information). These results indicate a surface-associated binding mode under these conditions. In the presence of CHOL and at high peptide concentration, however, the N-terminus of the peptide has been already shown deeply membrane inserted, but with the C-

terminus located near the polar headgroup region. Thus, CHOL tends to stabilize a peptide orientation perpendicular to the membrane surface.

Not only the presence of CHOL but also a high peptide concentration is needed to stabilize the transmembrane orientation. For CHOL-containing membranes, the intensity of the deuterium modulation observed for 5 mol % FTOAC-1 is about 2.2 times lower as compared to that at 0.5 mol % peptide concentration, while the peak intensity for FTOAC-8 is independent of concentration (Table 1). Thus, peptide orientation is dependent on the presence of CHOL as well as on peptide concentration. An analogous effect of  $A_N$  decrease was previously observed for trichogin GA IV in DPPC<sup>10</sup> and POPC<sup>16</sup> membranes.

It is worth mentioning that the amplitudes of the lines,  $A_N$ , in the presence and absence of CHOL shown in Table 1 are not the same. The larger values shown for CHOL-containing membranes (compared to those for CHOL-free membranes at the same peptide concentration) can be easily understood from the CHOL dependence of the water permeation profiles.<sup>21</sup> For membranes containing equimolar CHOL, the total change in polarity, greater than that for membranes without CHOL, decreases the permeability barrier by a factor of 2. For this reason, we are allowed to compare only data obtained for the same membrane composition (otherwise, the numerical comparison between different peptide concentrations would be incorrect). As we have seen above, however, such a problem does not arise for spectra obtained using CHOL- $d_7$ .

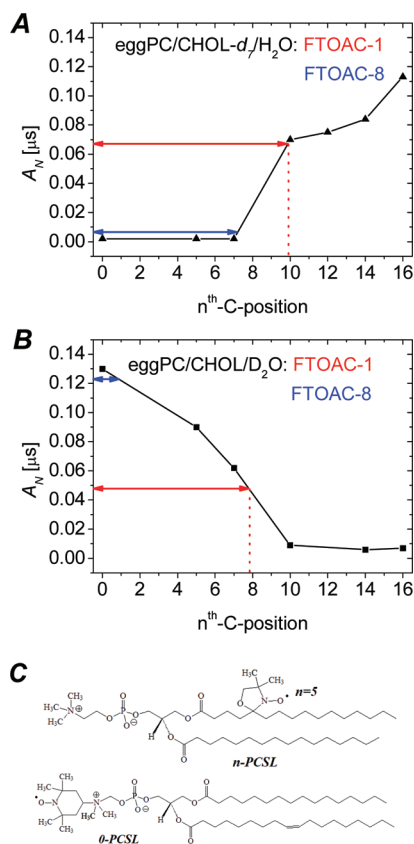


**Figure 3.** To determine the membrane immersion depths of the site-specifically spin-labeled peptide molecules, the values of the deuterium modulation amplitudes,  $A_N$ , shown in the ordinates and obtained in eggPC/CHOL- $d_7$ /H $_2$ O (A) and eggPC/CHOL/ $\text{D}_2\text{O}$  (B), respectively, are compared (by arrows) with the corresponding  $A_N$  values for a set of spin-labeled lipids ( $n = 0, 5, 7, 10, 12, 14$ , and 16). It is shown that the  $A_N$  value for 5 mol % FTOAC-1 in panel A corresponds to the 10th-lipid carbon position, while the modulation amplitude obtained for 5 mol % FTOAC-1 in panel B corresponds to the 8th-lipid carbon position. Panel C shows the chemical formulas of the spin-labeled lipids used.

**Table 1. Amplitudes,  $A_N$  ( $\mu\text{s}$ ), of the Fourier Transformation Spectra (Figure 3) for the Spin-Labeled Trichogin GA IV Analogues in Membranes Hydrated by  $\text{D}_2\text{O}$**

	FTOAC-1 0.5 mol %	FTOAC-8 0.5 mol %	FTOAC-1 5 mol %	FTOAC-8 5 mol %
eggPC	0.065	0.061	0.062	0.062
eggPC/ CHOL	0.118	0.120	0.053	0.123

According to the  $\text{D}_2\text{O}$ -polarity profile (Figure 3B) the  $A_N$  value obtained for 5 mol % FTOAC-1 corresponds approximately to the peak amplitude observed for the eighth-lipid carbon (thus, apparently two lipid carbons less than those obtained with the CHOL- $d_7$  calibration method). The larger modulation amplitude found using the  $\text{D}_2\text{O}$  method may be ascribed to experimental uncertainty and/or special resolution of the ESEEM technique.<sup>14</sup> As will be discussed below, it may also be explained by a contribution of peptide-associated  $\text{D}_2\text{O}$  molecules.

To ensure that disruption of the membrane bilayers does not occur, we compared the  $\text{D}_2\text{O}$  membrane permeation profiles in the absence and presence of 5 mol % of unlabeled peptide for

the same set of spin-labeled lipids (data not shown). Since we did not find any significant difference, we conclude that trichogin GA IV does not markedly disturb the membrane structure. This finding agrees with previously reported light-scattering experiments.<sup>22</sup> However, it is evident that peptide-induced lipid packing defects at local membrane sites cannot be ruled out.

**Peptide Aggregation.** To examine the influence of CHOL on peptide aggregation in eggPC membranes, CW EPR spectra were obtained for the two trichogin GA IV analogues in CHOL-free and CHOL-containing membranes (Figure 4).

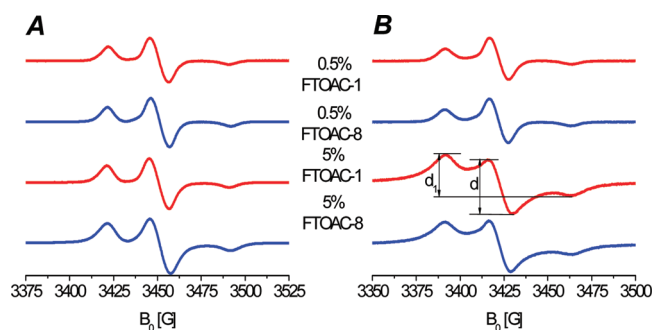


**Figure 4.** CW EPR spectra of the spin-labeled trichogin GA IV analogues in eggPC membranes (at 78.5 K) without CHOL (A) and with CHOL (B). All spectra are normalized by the amplitude of the central line and shifted downward for convenience. The parameters  $d_1$  and  $d$  (shown in panel B) were used for calculation of the interspin distances.

Each spectrum is characterized by three lines, corresponding to three possible  $m$  projections,  $m = 1, 0, -1$ , of the  $^{14}\text{N}$  spins onto its quantization axis. As at low-temperature EPR spectra are not sensitive to molecular motions, the position of each line is determined by the anisotropy of the  $g$ - and  $h$ fi-tensors. Only a slight broadening of the spectra of FTOAC-1 and FTOAC-8 is seen upon raising peptide concentration in CHOL-free membranes. However, in CHOL-containing membranes a significant broadening is observed for samples at high peptide concentration. The broadening of the FTOAC-1 spectrum appears to be slightly larger than that of FTOAC-8, as indicated by the lower amplitude of the central component in the former. Broadening of the spectra is caused by intermolecular spin–spin interactions due to peptide self-aggregation. The only interaction which can cause such broadening is a dipolar type of interaction, which is related to spin–spin distances. In this work, we did not determine the number of molecules,  $N$ , per aggregate. However, by assuming the minimum  $N = 2$ , one can estimate the intermolecular distances  $r$  from the calculated line shape. The central component is the narrowest one in the spectrum, so broadening results in its apparent decrease compared to the two other components, which is immediately seen by comparing the parameters  $d_1$  and  $d$  shown in Figure 4B. From these parameters we evaluated the value of the broadening as 2–3 G. Ascribing this value to the magnetic dipole–dipole interaction, one may roughly estimate the distances between two labels as  $\sim 2$  nm (for FTOAC-1 the distances are slightly less than that for FTOAC-8).

## DISCUSSION

**Role of CHOL on Peptide Membrane Insertion.** One of the most important results of our ESEEM experiments

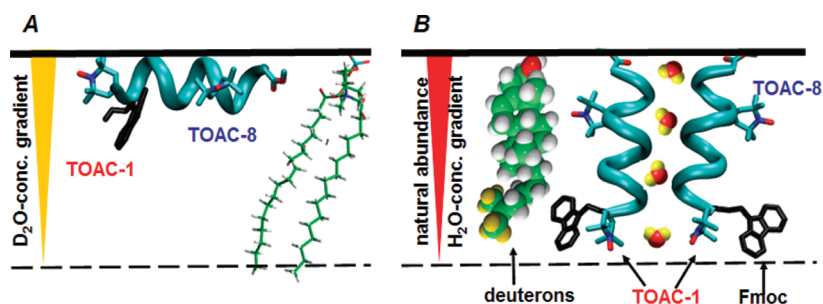


**Figure 5.** Representation of two different binding modes of the spin-labeled analogues of trichogin GA IV depicted at the outer leaflet of the lipid bilayer (for clarity, but in contrast with the experiment, both TOAC labels are shown in each peptide.) (A) The orientation of the peptide, indicated by a ribbon structure and shown parallel to the membrane surface, agrees with the experimentally determined water ( $D_2O$ ) accessibilities of both spin-labels at 0.5 mol % peptide/eggPC, 0.5 mol % peptide/eggPC/CHOL and 5 mol % peptide/eggPC. (B) At 5 mol % peptide concentration and in the presence of CHOL- $d_7$ , the helical molecules turn to a perpendicular orientation. Membrane insertion is accompanied by self-aggregation of parallelly aligned molecules. The polar ester group at the C-terminus of each peptide molecule as well as the polar CHOL hydroxyl group (both shown red colored) are most likely situated at the polar interface of the membrane. Note that the total length the peptide helix matches closely the thickness of the outer leaflet of the eggPC membrane bilayer. The immersion depth of the N-terminal FTOAC-1 spin-label was unambiguously determined due to the nearby presence of the deuterons of the hydrophobic alkyl side chain of CHOL- $d_7$ . In a separate experiment, but by using the eggPC/CHOL/ $D_2O$  approach, the insertion depth of the N-terminal spin-label was also determined at 5 mol % peptide concentration. The mismatch between the different insertion depths is explained on the basis of a slightly higher water concentration near the peptide, as compared to the extremely low water concentration in other regions of the inner core of the membrane (see text).

described in this study is the CHOL dependence of peptide penetration into eggPC membranes. This finding is achieved by site-specific spin-labeling of the peptide and determination of the positions of these spin-labels within the membrane. Information about the spin-label position is obtained by application of two complementary methods, which are distinguished by different distributions of the deuterium atoms in the membrane. One of the new methods to calibrate the immersion depths reported in this paper is based on the deeply membrane buried deuterium alkyl group of CHOL- $d_7$  (1.5 nm) attached to one side of the rigid polycyclic moiety of CHOL with a polar hydroxyl group at the opposite side (Figure 5). It is generally believed that the CHOL molecules are sandwiched between lipid molecules, with the polar hydroxyl group located at the headgroup of the membrane and the alkyl chain situated in the core of the lipid bilayer. Indeed, this perpendicular orientation of CHOL is confirmed by our measurements of deuterium-dependent modulations for a set of spin-labeled lipids in eggPC/CHOL- $d_7$ / $H_2O$  membranes (Figure 3A; Figure 4S, Supporting Information).

Clearly, the modulation data obtained for 5 mol % FTOAC-1/CHOL- $d_7$ / $H_2O$  provide strong evidence for the N-terminal TOAC-1 label located near the core of the membrane (Figures 3A and 5B). According to the calibration curve, the position of the TOAC-1 spin-label would correspond to the 10th-lipid carbon atom, at the depth of  $\sim 1.2$  nm. Thus, this residue would be slightly less deeply inserted than the deuterated isopropyl group of cholesterol ( $\sim 1.5$  nm). However, given the length of the peptide molecule ( $\sim 1.9$  nm),<sup>23</sup> the position of the TOAC-1 label would be expected located at a much deeper level in the membrane interior. At this point, it is important to recall that eggPC membranes are composed of a mixture of lipids of different lengths (34% C16:0; 2% C16:1; 32% C18:1; 18% C18:2, and 3% 20:4). Because the average length of the eggPC lipids is significantly greater than that of the lipid used for calibration (C16:1), it might be plausible that the  $A_N$  value for TOAC-1 might be out of the range of the calibration curve. In conclusion, TOAC-1 might be situated either above or more likely below the level of the deuterated region of CHOL- $d_7$ . In

any case, the observed  $A_N$  value is indicative of a deeply membrane buried N-terminus of the peptide.<sup>22</sup>

The long axes of both peptide and CHOL molecules are most likely parallelly aligned with respect to the membrane normal. Support to this view is given by (i) similar lengths of peptide and CHOL, (ii) similar positions of the peptide N-terminus and the CHOL alkyl side chain near the core of the membrane, and (iii) similar positions of the polar groups (the ester group at the C-terminus of the peptide and the hydroxyl group of CHOL) hydrogen bonded to the headgroup region of the membrane (Figure 5).

In contrast with our experiments at high peptide concentration, we did not detect any significant modulation for both spin-labeled peptides at low concentration in eggPC/CHOL- $d_7$ / $H_2O$  membranes. As discussed below, under the latter conditions the molecules are located parallel to the membrane surface. Also, our data obtained from spin-labeled peptides hydrated in  $D_2O$ , but from CHOL-lacking membranes are in line with such a surface-associated model. Thus, the experimental conditions used here to mimic the toxic effects of trichogin GA IV to mammalian cells, at relatively high peptide concentrations, explain clearly the important role played by CHOL on the penetration of peptide into the membrane.

The data from our EPR investigation are in excellent agreement with the results of a fluorescence quenching investigation using labeled trichogin GA IV in eggPC/CHOL vesicles.<sup>22</sup> Although no information about the peptide-membrane molecular orientation was offered in that study (since only one position of the peptide chain was labeled), the reported details for phenomenon of membrane insertion upon raising peptide concentration to 5 mol % compare well with our present findings.

#### Water Accessibility of Membrane Inserted Peptide.

Information about water accessibilities of the spin-labels was extracted from our ESEEM experiments with  $D_2O$  hydrated membranes. At low peptide concentration, in membranes with and without CHOL, similar and rather large  $A_N$  values were found for different spin-labeled trichogin GA IV analogues, which indicate a high level of water accessibility. This result



confirms that the molecules are positioned parallel to the polar membrane surface.

Upon raising the peptide concentration to 5 mol % and in the presence of CHOL, the modulation for the N-terminal TOAC-1 label is weaker compared to that observed for FTOAC-8 (Figure 1A and Table 1). Thus, a more deeply membrane buried N-terminus determined in this manner is in accord with the experiments performed with CHOL-*d*<sub>7</sub>/H<sub>2</sub>O membranes.

According to the  $A_N$  value obtained with CHOL/D<sub>2</sub>O membranes, however, the position of the TOAC-1 label corresponds roughly to the eighth lipid carbon positions, thus at least two lipid carbons less than that obtained with the CHOL-*d*<sub>7</sub> calibration method. The discrepancy between the insertion depths obtained by the two different methods may be induced by the experimental uncertainty of the ESEEM approach. The other explanation is that the water accessibility of the TOAC-1 label is higher than that expected based on the extremely low water concentration known to occur at this level of membrane depth, but in the absence of peptide. The higher water accessibility is therefore likely related to the presence of peptide-associated water molecules in that region of the membrane (Figure 5). Obviously, this proposed "water channel" should be further validated, but nonetheless the present results may give a clue for further investigations.

According to theoretical analyses, the ESEEM line shape of the Fourier-transformation spectra is determined by the dipolar anisotropic hyperfine interaction as well as by the nuclear quadrupole interaction between the unpaired electron and the deuterium nuclei. It may manifest itself in the sum of broad line and a narrow one with a doublet quadrupole splitting.<sup>9,14</sup>

The experimental lines of the spectra in eggPC/CHOL/D<sub>2</sub>O, shown in Figure 2, consist of a narrow line ( $A_N$ ) and a quadrupole doublet ( $\Delta$ ). Both  $A_N$  and  $\Delta$  are associated with free D<sub>2</sub>O molecules at a distance of 0.5–1 nm.  $A_N$  and  $\Delta$  are nonlinearly and linearly dependent on the water concentration, respectively.<sup>14</sup> For the FTOAC-1 label both the  $A_N$  and  $\Delta$  values decrease about 1.6 times upon increasing peptide concentration, while for FTOAC-8 these values remain unchanged. At the same time, for the FTOAC-1 spin-label the narrow line does not completely disappear at high peptide concentration. On the basis of this finding, one may also assume that some water molecules are located near the spin-label (Figure 5).

**Role of CHOL on Peptide Aggregation.** CW EPR results show that membrane insertion is coupled with peptide self-association. The line broadenings observed for FTOAC-1 and, although to a lower extent, for FTOAC-8 as well clearly suggest parallelly aligned peptide constituents in the aggregate.

Self-assembling of amphipathic peptides in membranes is a well-known phenomenon. Some peptides self-aggregate in an antiparallel manner due to (electrical) dipole–dipole stabilization of the complex.<sup>24</sup> In other cases, a parallel alignment is favored, depending on whether amino acid side chains able to stabilize the aggregate are present.<sup>17,25</sup> Here, the parallel alignment might be most likely determined by hydrogen bonds between the peptide C-terminal ester groups and the polar groups of the lipids, while association is favored by van der Waals interactions between hydrophobic peptide residues and surrounding lipid acyl chains which take place in the core of the membrane.

A survey of the literature on trichogin GA IV studied under different conditions shows a varying number of molecules

composing the aggregate:  $N = 2$  (DPPC, 77 K),<sup>10</sup>  $N = 4$  (hydrophobic solvent, 77 K),<sup>24,26</sup>  $N = 4$  (eggPC, 300 K),<sup>27</sup>  $N = 8$  (eggPC/CHOL, 300 K).<sup>6</sup> Also, a heterogeneity arising from different aggregation states in the membrane cannot be ruled out.<sup>6</sup>

The aggregates might not be necessarily bound to the outer membrane leaflet only, since fluorescence experiments clearly showed peptides bound at the outer as well as at the inner side of the bilayer surface, even at low peptide concentration where membrane leakage was found not to take place.<sup>8</sup> Based on an EPR study of trichogin GA IV in POPC, a "gramicidin A"-like transmembrane head-to-head associated dimer was proposed, with a total length matching the thickness of the membrane.<sup>16</sup> Trichogin GA IV was suggested to act as a hole-drilling device, influencing the packing of the surrounding lipid of the membrane. Thus, in view of the above literature data, our interpretation of the present CW EPR experiments which suggest a parallel alignment of two associated peptide molecules does not rule out the possibility of a tetramer, composed of two dimers, which are associated in a head-to-head manner spanning the total bilayer thickness.

**Role of CHOL on Antibiotic and Toxic Effects of Trichogin GA IV.** At low peptide concentration and in the absence of CHOL, the conditions that were chosen to mimic the antibiotic activity of trichogin GA IV, the peptide molecules are found monomolecularly distributed and associated with the surface of the membrane. From a previous PELDOR experiment of trichogin GA IV bound to the cell membrane of *Micrococcus luteus*, it was demonstrated that the peptide molecules are indeed distributed at the level of the cytoplasm membrane, but aggregates of peptide molecules were not detected.<sup>27</sup> From a fluorescence study performed under the same conditions, a weak K<sup>+</sup>/Na<sup>+</sup> selectivity was shown to take place for trichogin GA IV,<sup>28</sup> which suggests a favored transport of K<sup>+</sup> ions due to the relative small radius of hydrated K<sub>aq</sub><sup>+</sup> (compared to Na<sub>aq</sub><sup>+</sup>) molecules. The kinetics of membrane leakage was found much slower than that observed for the barrel-stave type of ion channels like those characterizing the peptaibiotics zervamicin and alamethicin.<sup>27</sup> Microscopic, meta-stable channels might probably be involved in the transport of small solutes across the bilayer, thereby disrupting the membrane potential and eventually forcing the bacterial cell to die. Similar observations were recently reported for the water interface between the antibiotic duramycin and phospholipid monolayers, revealed by label-free, vibrational sum-frequency generation spectroscopy.<sup>29</sup> Unfortunately, the CHOL dependence of our presently described ESEEM method does not provide data on the presence of peptide-associated water in CHOL-lacking membranes.

At high peptide concentration, trichogin GA IV was shown to be toxic for mammalian cells.<sup>30</sup> From a fluorescence study, it was suggested that at high peptide and CHOL concentrations, this lipopeptide is able to induce even membrane leakage of larger molecules like carboxyfluorescein (Figure 1S, Supporting Information) due to a pore-, rather than to a detergent-, carpet-, or toroidal-type mechanism.<sup>6</sup> The results of our present ESEEM experiments performed under these conditions agree nicely with the ability of trichogin GA IV to form trans-membrane aggregates, which are likely inducing (micro)-water channels across the lipid bilayer.

## CONCLUSION

In this work, we investigated the role of CHOL on the mammalian membrane leakage (toxic) effects of the antibiotic lipopeptide trichogin GA IV in CHOL-free and CHOL-containing eggPC membranes by two different ESEEM calibration methods. The study of the two spin-labeled analogues examined showed two different binding modes to the membrane which were found dependent on the CHOL presence. In the absence of CHOL, the peptides are bound to the membrane surface, even at high peptide concentration. By contrast, in the presence of CHOL, upon raising the peptide concentration, the molecules of the latter move from a mode parallel to the membrane surface to a membrane-inserted mode. Broadening of the CW EPR lines of the spectra of the N-terminal as well as the C-terminal labeled analogues indicated that peptide membrane insertion is accompanied by self-aggregation. The peptide molecules in the aggregate were found aligned in a parallel disposition. Both CHOL molecules and peptide aggregates are most likely sandwiched between the lipid molecules. Here, ESEEM spectroscopy, combined with two different deuterium labeling techniques, is demonstrated to be potentially useful for the determination of the location as well as the water accessibility of membrane-bound peptides and, by extension, of proteins as well.

## ASSOCIATED CONTENT

### Supporting Information

Chemical structures for the compounds used in this work and additional ESEEM data. This material is available free of charge via the Internet at <http://pubs.acs.org>.

## AUTHOR INFORMATION

### Corresponding Author

\*E-mail: J.Raap@Chem.LeidenUniv.NL.

### Present Address

<sup>†</sup>Leiden Institute of Chemistry, University of Leiden, 2300RA Leiden, The Netherlands.

### Notes

The authors declare no competing financial interest.

## ACKNOWLEDGMENTS

The authors are grateful to Dr. A. D. Milov for useful discussions. This work was supported by the Ministry of Education and Science of Russian Federation (14.740.11.0369 and 11.519.11.1006), The Netherlands Organization of Scientific Research (NWO 047.017.034), and the MIUR of Italy (PRIN 2008).

## REFERENCES

- (1) Toniolo, C.; Crisma, M.; Formaggio, F.; Peggion, C.; Epand, R. F.; Epand, R. M. *Cell. Mol. Life Sci.* **2001**, *58*, 1179–1188.
- (2) Auvin-Guette, C.; Rebuffat, S.; Prigent, Y.; Bodo, B. *J. Am. Chem. Soc.* **1992**, *114*, 2170–2174.
- (3) Toniolo, C.; Peggion, C.; Crisma, M.; Formaggio, F.; Shui, X.; Eggleston, D. S. *Nat. Struct. Biol.* **1994**, *1*, 908–914.
- (4) Peggion, C.; Formaggio, F.; Crisma, M.; Epand, R. F.; Epand, R. M.; Toniolo, C. *J. Pept. Sci.* **2003**, *9*, 679–689.
- (5) Monaco, V.; Locardi, E.; Formaggio, F.; Crisma, M.; Mammi, S.; Peggion, E.; Toniolo, C.; Rebuffat, S.; Bodo, B. *J. Pept. Res.* **1998**, *52*, 261–272.
- (6) Stella, L.; Mazzuca, C.; Venanzi, M.; Palleschi, A.; Didonè, M.; Formaggio, F.; Toniolo, C.; Pispisa, B. *Biophys. J.* **2004**, *86*, 936–945.
- (7) Bocchinfuso, G.; Palleschi, A.; Orioni, B.; Grande, G.; Formaggio, F.; Toniolo, C.; Park, Y.; Hahm, K.-S.; Stella, L. *J. Pept. Sci.* **2009**, *15*, 550–558.
- (8) Mazzuca, C.; Orioni, B.; Coletta, M.; Formaggio, F.; Toniolo, C.; Maulucci, G.; De Spirito, M.; Pispisa, B.; Venanzi, M.; Stella, L. *Biophys. J.* **2010**, *99*, 1791–1800.
- (9) Erilov, D. A.; Bartucci, R.; Guzzi, R.; Shubin, A. A.; Maryasov, A. G.; Marsh, D.; Dzuba, S. A.; Sportelli, L. *J. Phys. Chem. B* **2005**, *109*, 12003–12013.
- (10) Salnikov, E. S.; Erilov, D. A.; Milov, A. D.; Tsvetkov, Yu. D.; Peggion, C.; Formaggio, F.; Toniolo, C.; Raap, J.; Dzuba, S. A. *Biophys. J.* **2006**, *91*, 1532–1540.
- (11) Carmieli, R.; Papo, N.; Zimmermann, H.; Potapov, A.; Shai, Y.; Goldfarb, D. *Biophys. J.* **2006**, *90*, 492–505.
- (12) Gordon-Grossman, M.; Gofman, Y.; Zimmermann, H.; Frydman, V.; Shai, Y.; Ben-Tal, N.; Goldfarb, D. *J. Phys. Chem. B* **2009**, *113*, 12678–12695.
- (13) Gordon-Grossman, M.; Zimmermann, H.; Wolf, S. G.; Shai, Y.; Goldfarb, D. *J. Phys. Chem. B* **2012**, *116*, 179–188.
- (14) Milov, A. D.; Samoilova, R. I.; Shubin, A. A.; Grishin, Yu. A.; Dzuba, S. A. *Appl. Magn. Reson.* **2008**, *35*, 73–94.
- (15) Milov, A. D.; Samoilova, R. I.; Shubin, A. A.; Gorbunova, E. Yu.; Mustaeva, L. G.; Ovchinnikova, T. V.; Raap, J.; Tsvetkov, Yu. D. *Appl. Magn. Reson.* **2010**, *38*, 75–84.
- (16) Syryamina, V. N.; Isaev, N. P.; Peggion, C.; Formaggio, F.; Toniolo, C.; Raap, J.; Dzuba, S. A. *J. Phys. Chem. B* **2010**, *114*, 12277–12283.
- (17) Milov, A. D.; Samoilova, R. I.; Tsvetkov, Yu. D.; De Zotti, M.; Formaggio, F.; Toniolo, C.; Handgraaf, J.-W.; Raap, J. *Biophys. J.* **2009**, *96*, 3197–3209.
- (18) Dikanov, S. A.; Tsvetkov, Yu. D. In *Electron Spin Echo Envelope Modulation (ESEEM) Spectroscopy*; CRC Press: Boca Raton, FL, 1992; p 142.
- (19) Monaco, V.; Formaggio, F.; Crisma, M.; Toniolo, C.; Hanson, P.; Millhauser, G. L. *Biopolymers* **1999**, *50*, 239–253.
- (20) Venanzi, M.; Gatto, E.; Bocchinfuso, G.; Palleschi, A.; Stella, L.; Baldini, C.; Formaggio, F.; Toniolo, C. *J. Phys. Chem. B* **2006**, *110*, 22834–22841.
- (21) Marsh, D. *Proc. Natl. Acad. Sci. U. S. A.* **2001**, *98*, 7777–7782.
- (22) Mazzuca, C.; Stella, L.; Venanzi, M.; Formaggio, F.; Toniolo, C.; Pispisa, B. *Biophys. J.* **2005**, *88*, 3411–3421.
- (23) Milov, A. D.; Erilov, D. A.; Salnikov, E. S.; Tsvetkov, Yu. D.; Formaggio, F.; Toniolo, C.; Raap, J. *J. Phys. Chem. Chem. Phys.* **2005**, *7*, 1794–1799.
- (24) Milov, A. D.; Tsvetkov, Yu. D.; Formaggio, F.; Crisma, M.; Toniolo, C.; Raap, J. *J. Am. Chem. Soc.* **2000**, *122*, 3843–3848.
- (25) Milov, A. D.; Tsvetkov, Yu. D.; Formaggio, F.; Crisma, M.; Toniolo, C.; Millhauser, G. L.; Raap, J. *J. Phys. Chem. B* **2001**, *105*, 11206–11213.
- (26) Milov, A. D.; Tsvetkov, Yu. D.; Formaggio, F.; Crisma, M.; Toniolo, C.; Raap, J. *J. Am. Chem. Soc.* **2000**, *122*, 3843–3848.
- (27) Kropacheva, T. N.; Raap, J. *Biochim. Biophys. Acta* **2002**, *1567*, 193–203.
- (28) Milov, A. D.; Samoilova, R. I.; Tsvetkov, Yu. D.; Gusev, V. A.; Formaggio, F.; Crisma, M.; Toniolo, C.; Raap, J. *Appl. Magn. Reson.* **2002**, *23*, 81–95.
- (29) Rzeznicka, I. I.; Sovago, M.; Backus, E. H. G.; Bonn, M.; Yamada, T.; Kobayashi, T.; Kawai, M. *Langmuir* **2010**, *26*, 16055–16062.
- (30) Toniolo, C.; Crisma, M.; Formaggio, F.; Peggion, C.; Monaco, V.; Goulard, C.; Rebuffat, S.; Bodo, B. *J. Am. Chem. Soc.* **1996**, *118*, 4952–4958.